

Influence of voltammetric parameters on Zn–Ni alloy deposition under potentiodynamic conditions

A. Petrauskas · L. Grincevičienė · A. Češūnienė

Received: 4 July 2008 / Accepted: 17 February 2009 / Published online: 5 March 2009
© Springer Science+Business Media B.V. 2009

Abstract The phase composition of Zn–Ni alloys electrodeposited from acetate-chloride plating solutions containing Zn^{+2} and Ni^{+2} ions at ratio of 1–12.8 at 50 °C was investigated by the potentiodynamic stripping method. Two anodic current density (i_a) peaks emerged in potentiodynamic stripping curves (PDC) at $E < 0.0$ V and $E > 0.0$ V (vs. $\text{Ag}/\text{AgCl}/\text{KCl}_{\text{sat}}$), that were attributed to oxidation of certain phases of the Zn–Ni alloy. The ratio of these phases in deposited Zn–Ni alloys under potentiodynamic conditions was affected by the potential sweep rate (v) and maximum cathodic current density (i_c). The ratio of Zn and Ni in certain phases of Zn–Ni alloy was determined by the partial potentiodynamic stripping technique. Experimental data show that Zn–Ni alloy, containing 6.5 at.% Zn and 93.5 at.% Ni and dissolved in i_a peak H ($E > 0.0$ V), provides the black coloration of the Zn–Ni alloy.

Keywords Electrodeposition · Zn–Ni alloy · Temperature · Cyclic voltammetry · Partial potentiodynamic stripping · Acetate-chloride electrolyte

1 Introduction

Studies of Zn–Ni codeposition can be divided into two categories: investigation of regularities of both normal and anomalous Zn–Ni codeposition and determination of phase compositions of Zn–Ni alloys using XRD and the potentiodynamic stripping method.

Normal and anomalous Zn–Ni codeposition is determined by numerous factors, such as cathodic current density i_c [1], the electrodeposition potential (E_c) [2, 3], the ratio of Zn^{+2} and Ni^{+2} ions in the electrolyte, as well as pH and temperature of the solution [4–7]. Literature reports mostly deal with conditions for normal and anomalous codeposition and do not investigate the codeposition mechanism. The influence of metal hydroxides on codeposition of Zn–Ni alloy was investigated by Chi-Chang Hu et al. [8]. Codeposition of Zn–Ni alloy is accompanied by the discharge of H^+ ions, which increases the pH near the cathode surface and facilitates formation of basic metal compounds. Cyclic voltammetry experiments indicated that adsorption, desorption, and reduction of basic metal compounds on the surface determines whether normal or anomalous codeposition will take place [8].

Investigation of the phase composition of Zn–Ni alloys is performed by XRD and classical anodic stripping voltammetry [4, 6, 9–16]. In some cases both methods were combined. Typically four anodic current i_a peaks A, B, C and D emerge in potentiodynamic curves (PDC) upon stripping [11–13, 15]. These i_a peaks are attributed to dissolution of Zn from different phases of Zn–Ni alloy and reveal the phase composition. Peak A being in the most negative range of potentials corresponds to anodic dissolution of Zn from η -phase. This phase represents a solid solution of 1% Ni in Zn [11]. Peak B is attributed to dissolution of Zn from α -phase, which is a solid solution of Zn in Ni of varying composition. The composition of this phase can vary in a wide range of Zn concentration (up to 30 at.%). Peak C is attributed to dissolution of Zn from γ -phase ($\text{Ni}_5\text{Zn}_{21}$). Peak D is typically attributed to the anodic dissolution of active porous Ni as it is believed that all of Zn has already dissolved at more negative potentials [11]. New cyclic voltammetry and partial potentiodynamic

A. Petrauskas (✉) · L. Grincevičienė · A. Češūnienė
Institute of Chemistry, Electrochemistry of Metals, Goštauto 9,
01108 Vilnius, Lithuania
e-mail: acenin@ktl.mii.lt

stripping data [17] indicate that under galvanostatic conditions (at 20 °C, ratio $[\text{Zn}^{+2}]/[\text{Ni}^{+2}] = 1:6.4$) peak D can be assigned to oxidation of Zn–Ni alloy containing 42.4 at.% of Zn and 57.6 at.% Ni.

During potentiodynamic stripping of Zn–Ni alloy deposited in the above mentioned plating solution under galvanostatic conditions at 50 °C stripping PDC exhibited i_a peaks at $E < 0.0$ V and at $E > 0.0$ V [18]. Analogous data were obtained by investigating Zn–Ni alloys deposited in a plating solution with the ratio $[\text{Zn}^{+2}]/[\text{Ni}^{+2}] = 1:83$ under galvanostatic conditions at 20 °C [17]. Anodic current peak at $E > 0.0$ V is in the same potential range as that of i_a peak for Ni oxidation. Therefore, a question might come to mind about what process takes place in this anodic peak, whether it is dissolution of porous Ni or dissolution of Zn–Ni alloy? The authors [6] did not observe a i_a peak at $E > 0$ V in the potentiodynamic stripping curves because they examined coatings deposited in a plating solution with the ratio of $[\text{Zn}^{+2}]/[\text{Ni}^{+2}] = 1: 6.4$ at 40 °C.

The mechanism of electrolytic Zn–Ni alloy deposition has been thoroughly investigated in sulphate [1, 2], chloride [3, 11, 12, 18], and sulphate-chloride plating solutions and only a few reports are available for acetate-sulphate and acetate-chloride plating solutions [17–20].

Some work has been done on the regularity of codeposition of alloys and the phase composition of deposited alloys by cyclic voltammetry. When the anodic dissolution potentials for different phases are well separated anodic potentiodynamic stripping allows determination of the composition of dissolving alloys. If anodic dissolution potentials for different phases are too close to each other then only very small quantities of alloy are deposited, in order to avoid overlapping of i_a peaks. When extremely thin alloy films are used, it becomes difficult to determine the phase and elemental composition by other standard methods.

Alloys deposited under galvanostatic, potentiostatic, and potentiodynamic conditions can be used for investigation of phase composition.

As a rule, all known phases are found in alloy films deposited under galvanostatic conditions. Keeping the thickness of alloy films and other conditions the same, the ratio of various phases depends only on i_c .

Electrodeposition of alloys under potentiostatic conditions forms only those phases that can be deposited at a given potential (or at more positive potentials).

The potentiodynamic deposition and the potentiodynamic anodic stripping methods are also widely used [11, 13]. All phases of Zn–Ni alloy are detected in films deposited under potentiodynamic conditions [17].

In this work we used a modified method of partial potentiodynamic stripping, meaning that the potential was swept up to certain values so that some phase or phases would be completely removed from the film. Using partial

potentiodynamic stripping it was possible to accumulate larger quantities of certain phases on the electrode. Figure 1 clearly demonstrates how partial potentiodynamic stripping allows one to accumulate one (Fig. 1a) or two phases (Fig. 1b) on the cathode. Partial potentiodynamic stripping method can be realized only under conditions of potentiodynamic deposition and anodic stripping. In industry, however, exclusively galvanostatic deposition is used. The aim of this work was, therefore, to establish the effect of different parameters on Zn–Ni alloy deposition under potentiodynamic conditions and compare them with data obtained for alloys deposited under potentiostatic and galvanostatic conditions. Temperature of 50 °C and the ratio $[\text{Zn}^{+2}]/[\text{Ni}^{+2}] = 1:12.8$ were chosen because black Zn–Ni alloy can be deposited under these conditions without additives.

2 Experimental

Potentiodynamic studies were conducted in a thermostated two compartment electrochemical cell ISE-2 using a potentiostat PI50-1. 1 cm² Pt electrode was used as working electrode. Pure Ni foil was used as anode. The anode was separated from the cathode by a diaphragm. The following salts were used to prepare solutions: Ni(CH₃COO)₂ · 4H₂O; ZnCl₂; KCl; H₃BO₃ and HCl. All substances used were at least of pro analysis grade. The Zn–Ni alloys were deposited from acetate-chloride plating solution containing 0.56 M Ni(CH₃COO)₂ · 4H₂O, 0.91 M KCl, 0.5 M H₃BO₃, and 0.029 M ZnCl₂ (the ratio $[\text{Zn}^{+2}]/[\text{Ni}^{+2}] = 1:12.8$) under cyclic voltammetry conditions at 50 °C.

A 50% solution of ZnCl₂ was prepared by dissolving a whole prepacked bag of precise weight in bidistilled water, and then the required quantity of it was added to the above mentioned plating solution. Potentiodynamic stripping of Zn–Ni alloys deposited under galvanostatic and cyclic voltammetry conditions were performed in an acetate-chloride plating solution. The electrolyte was not agitated during either deposition or potentiodynamic stripping. Cyclic voltammetry was performed at pH = 5. All potentials are given relative to the saturated Ag/AgCl/KCl_{sat} electrode.

The charges Q_{cath} , Q_{anod} , Q_D and Q_H were calculated by integrating the charges transferred in cathodic and anodic processes or in i_a peaks D and H, respectively. The parts of charge transferred in the separate peaks D and H were calculated from the following equations:

$$Q_D[\%] = \frac{Q_D}{Q_D + Q_H} 100[\%]$$

$$Q_H[\%] = \frac{Q_H}{Q_D + Q_H} 100[\%]$$

The quantity of Zn and Ni in the alloy was determined by electron probe microanalysis (JXA-50A (JEOL)).

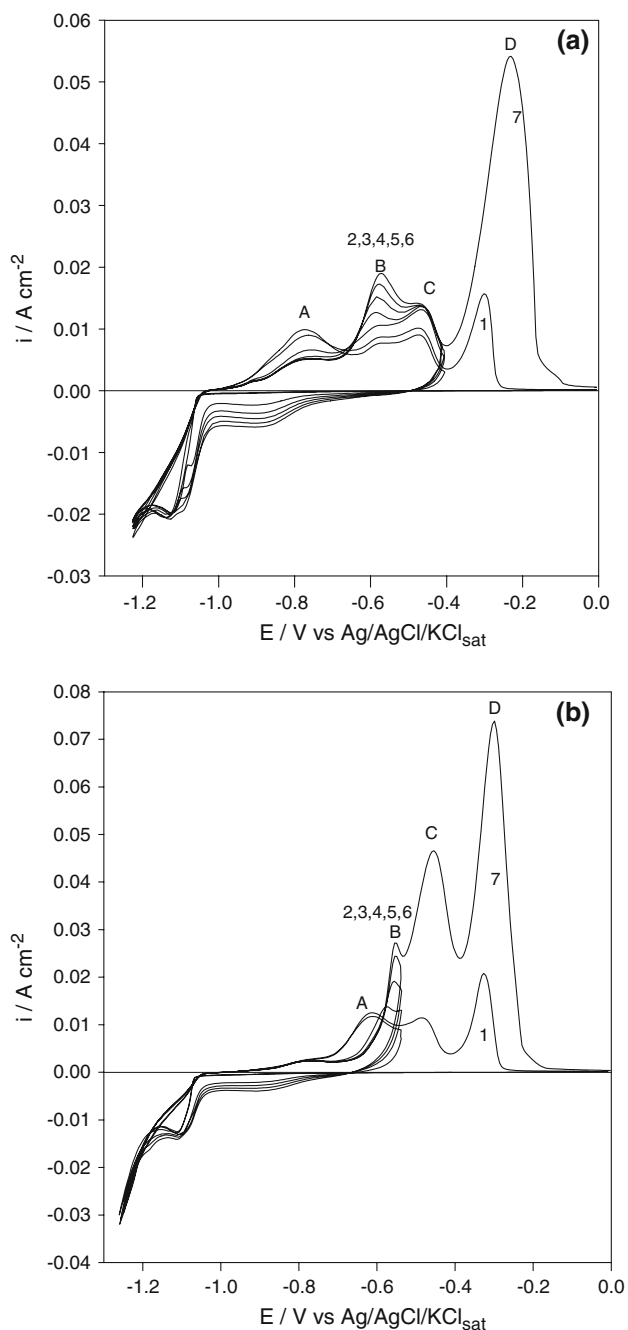


Fig. 1 Cyclic voltammograms of Zn–Ni alloys deposited in nickel plating solution containing $0.1385 \text{ mol l}^{-1}$ of ZnCl_2 on the Pt electrode. $t = 20 \text{ }^\circ\text{C}$, $\text{pH } 5$, $\nu = 0.005 \text{ V s}^{-1}$. **a** Curve 1: first cycle from the Pt potential, 0.3 to -1.25 V and back to 0.0 V . Curve 2: second cycle from 0.0 to -1.25 V and back to -0.4 V . Curves 3–6: third to sixth cycles from -0.4 to -1.25 V and back to -0.4 V . Curve 7: seventh cycle from -0.4 to -1.25 V and back to 0 V . **b** Curve 1: first cycle from the Pt potential, 0.3 to -1.25 V and back to 0.0 V . Curve 2: second cycle from 0.0 to -1.25 V and back to -0.53 V . Curves 3–6: third to sixth cycles from -0.53 to -1.25 V and back to -0.53 V . Curve 7: seventh cycle from -0.53 to -1.25 V and back to 0

The hardness of the alloys was measured using a hardness measurement device PMT-3 (the Vicker’s method) with a diamond pyramid loaded with a weight of 20 g .

3 Results and discussion

3.1 Dependence of physical and mechanical properties of Zn–Ni alloy on temperature

A mat, deep-grey Zn–Ni alloy containing $70.2 \text{ at.}\%$ Ni was deposited at $20 \text{ }^\circ\text{C}$ (Table 1). The quantity of Ni in the alloy increased up to $87.7 \text{ at.}\%$ with increase in deposition temperature up to $50 \text{ }^\circ\text{C}$, and the properties of the alloy changed significantly. It was shown that the hardness of alloy deposited at $50 \text{ }^\circ\text{C}$ was higher than that deposited at $20 \text{ }^\circ\text{C}$ (Table 1).

A bright black Zn–Ni alloy used for decorative finishing can be deposited on a bright Ni substrate in an acetate-chloride plating solution at $50 \text{ }^\circ\text{C}$. This suggests that the deposition temperature and i_c have a significant influence on the phase composition.

3.2 Studies of Zn–Ni alloy by cyclic voltammetry

3.2.1 Potentiostatic conditions

The data for the dependence of i_c on deposition time (τ) presented in Fig. 2 were collected under potentiostatic conditions. Maximum i_c values of 0.055 A cm^{-2} ; 0.04 A cm^{-2} , and 0.015 A cm^{-2} at E_c values -1.2 V ; -1.0 V , and -0.9 V were achieved after 8–10 s; 30 s, and 60 s, respectively. This showed that the cathodic process underwent changes during deposition and the phase composition, therefore, also varied. At more positive potentials it took longer for the cathodic process to stabilize under potentiostatic conditions. Change in phase composition with deposition time was confirmed by the potentiodynamic stripping data presented in Fig. 3. It was established that the quantity of phase dissolved in i_a peak H at

Table 1 Dependence of the hardness of Zn–Ni alloys and the quantity of Ni in alloys on deposition temperature and i_c

$t \text{ (}^\circ\text{C)}$	20 °C		50 °C	
$i_c \text{ (A cm}^{-2}\text{)}$	0.002	0.005	0.002	0.005
Ni (at.%)	70.2	80.8	87.7	82.9
Hardness (N mm ⁻²)	26.1	24.3	57.8	36.4

Coatings were deposited under galvanostatic conditions. Coating thickness was $15 \text{ }\mu\text{m}$

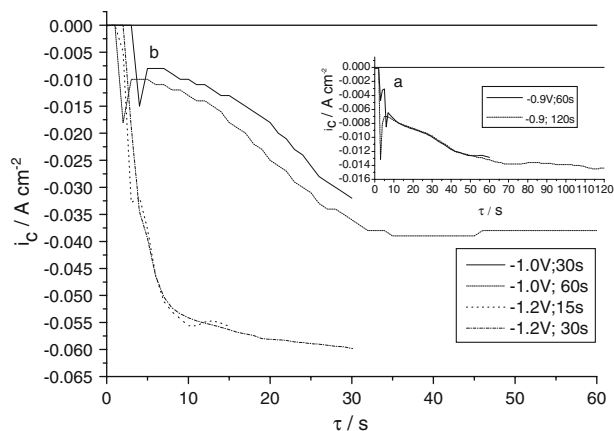


Fig. 2 Maximum cathodic current density versus deposition time. The data were obtained in acetate-chloride plating solution with the ratio $[Zn^{+2}]/[Ni^{+2}] = 1:12.8$ at different potentials on Pt electrode. $t = 50\text{ }^{\circ}\text{C}$, pH 5

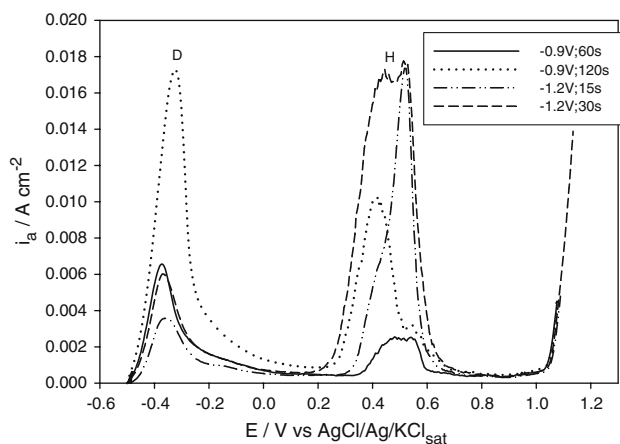


Fig. 3 Potentiodynamic stripping response ($v = 0.005\text{ V s}^{-1}$) of Zn–Ni alloys deposited in acetate-chloride plating solution with the ratio $[Zn^{+2}]/[Ni^{+2}] = 1:12.8$ at different potentials on Pt electrode. $t = 50\text{ }^{\circ}\text{C}$, pH 5

$E_a > 0\text{ V}$ increased with deposition time. The data presented in Table 2 show that at more negative potentials or at longer deposition times (at constant E_c) the greater

quantity of the phase, dissolved in i_a peak H, was present in Zn–Ni alloy. This observation is in line with literature data, which states that electrodeposition of Ni proceeds via basic metal compounds [8]. At higher rates of electrolysis the solution near the electrode surface becomes more alkaline and, thus, electrodeposition of Ni is facilitated.

3.2.2 Potentiodynamic conditions

The data obtained potentiodynamically showed that phase composition of Zn–Ni alloy deposited under galvanostatic conditions depended on deposition i_c [17]. The changes in phase composition of Zn–Ni alloy presented in Fig. 4 showed that phase composition of Zn–Ni alloy deposited under potentiodynamic conditions was greatly affected by maximum i_c , which was reached by sweeping the potential towards more negative potentials at constant v . Sweeping the potential until the maximum i_c of 0.02 A cm^{-2} was reached revealed that only a small portion of Zn–Ni alloy phase, dissolved at $E < 0.0\text{ V}$, was present (Fig. 4, curve 1). The phase, which was dissolved at $E > 0.0\text{ V}$, prevailed in the alloy when maximum i_c was increased up to 0.1 A cm^{-2} (Fig. 4, curve 5). The calculations (Table 3) showed that during potentiodynamic stripping of Zn–Ni alloy at $v = 0.005\text{ V s}^{-1}$ then maximum i_c grew from 0.02 A cm^{-2} to 0.1 A cm^{-2} Q_H increased from 2.3% up to 87.3%, Q_D decreased from 97.7% to 12.75% and the total current efficiency (CE_t) increased from 38.5% up to 85.1%. This is likely determined by the regularities of formation of basic metal compounds.

The data presented in Fig. 5 showed the influence of sweep rate v on anodic charge distribution in the potential regions of i_a peak of D (Q_D) and i_a peak H (Q_H). When v increased from 0.002 V s^{-1} to 0.01 V s^{-1} the value of i_a peaks H became greater. When v increased up to 0.05 V s^{-1} i_a peak C, which can be attributed to oxidation of α -phase or γ -phase of Zn–Ni alloy, emerged at $E = -0.6\text{ V}$ on the potentiodynamic curve (Fig. 5, Curve 4). Investigation showed that at maximum $i_c = 0.05\text{ A cm}^{-2}$ the ratio $Q_H[\%]/Q_D[\%]$ increased from 1.3 to 2.1 with

Table 2 Dependence of total current efficiency (CE_t) and charges Q_D and Q_H on cathodic potential (E_c) and deposition time (τ)

E_c (V)	Deposition time/s	Q_{cath}/C	Q_{anod}/C	CE_t (%)	Q_D/C (%)	Q_H/C (%)
–0.9	60	0.63	0.44	70	0.26 (60)	0.18 (40)
	120	1.46	1.06	73	0.57 (54)	0.49 (46)
–1.0	30	0.57	0.36	63	0.12 (32)	0.24 (68)
	60	1.79	1.44	80	0.21 (14.5)	1.23 (85.5)
–1.2	15	0.93	0.63	68	0.15 (24)	0.48 (76)
	30	1.67	1.25	75	0.22 (1.78)	1.03 (82.22)

Q_{cath} , total cathodic charge (from Fig. 2). Q_{anod} , total anodic charge (from Fig. 3). The data were obtained under potentiodynamic conditions ($v = 0.005\text{ V s}^{-1}$) at $50\text{ }^{\circ}\text{C}$

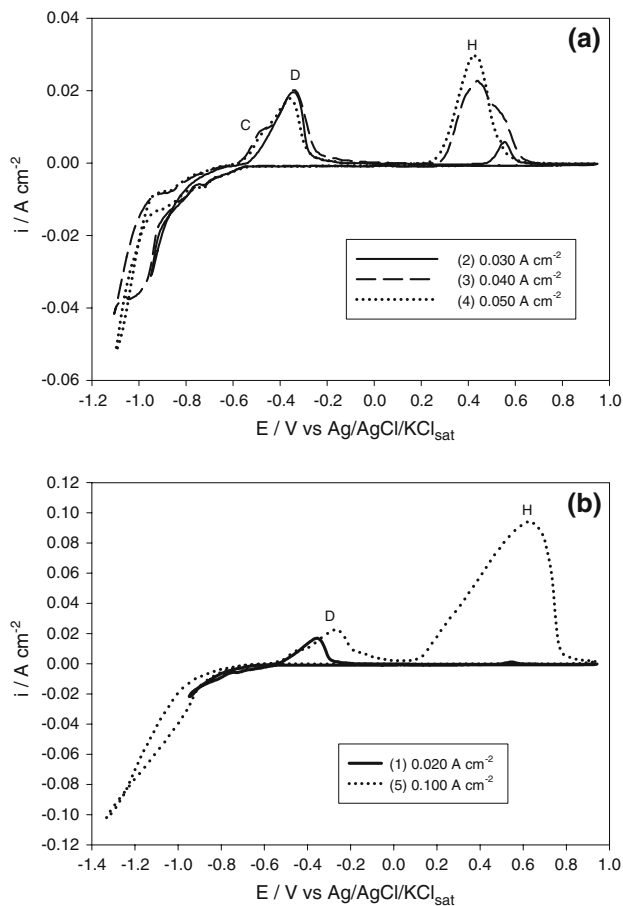


Fig. 4 Cyclic voltammety of Zn–Ni alloy deposited in acetate-chloride plating solution with the ratio $[Zn^{+2}]/[Ni^{+2}] = 1:12.8$ at $50\text{ }^\circ\text{C}$ at $\nu = 0.005\text{ V s}^{-1}$ on Pt electrode versus magnitude of maximal cathodic current density. pH 5

increase in ν from 0.002 V s^{-1} up to 0.05 V s^{-1} (Table 4). Variation in the potential sweep rate had a great influence on the total current efficiency (CE_t) of Zn–Ni alloy which decreased from 75.0% to 59.0% with increase in ν up to 0.05 V s^{-1} (Table 4).

Under potentiodynamic stripping conditions Zn from η -, α -, and γ - phases of Zn–Ni alloy dissolves within i_a peaks A, B, and C. Pure Ni matrix, thus, remains on the electrode and is dissolved in i_a peak D [11, 13]. The potentiodynamic

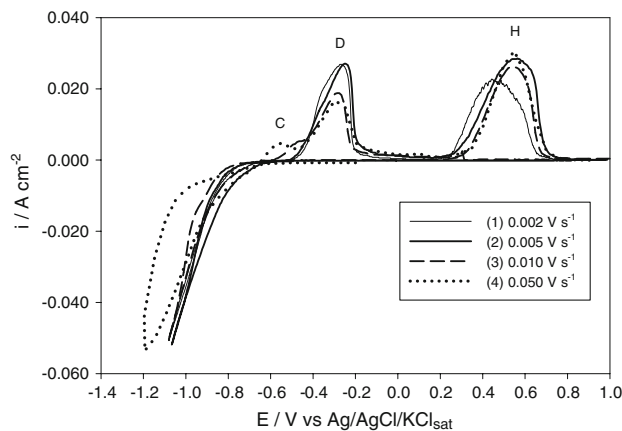


Fig. 5 Cyclic voltammety of Zn–Ni alloy deposited in acetate-chloride plating solution with the ratio $[Zn^{+2}]/[Ni^{+2}] = 1:12.8$ at $50\text{ }^\circ\text{C}$ on Pt electrode; deposition potential swept to $i_c = 0.050\text{ A cm}^{-2}$

Table 4 Influence of ν on Q_D , Q_H and CE_t

$\nu/\text{V s}^{-1}$	0.002	0.005	0.01	0.05
Q_D/C (%)	2.26 (43.0)	0.97 (37.7)	0.39 (39.0)	0.068 (32.0)
Q_H/C (%)	3.01 (57.0)	1.6 (62.3)	0.6 (61.0)	0.145 (68.0)
CE_t (%)	75.0	93.7	78.0	59.0

The data were obtained under cyclic voltammety conditions at $50\text{ }^\circ\text{C}$ when E_c was swept until maximum $i_c = 0.05\text{ A cm}^{-2}$

stripping response of alloy deposited from a plating solution with the ratio of $[Zn^{+2}]/[Ni^{+2}] = 1:12.8$ at $50\text{ }^\circ\text{C}$ exhibited i_a peak D at $E < 0.0\text{ V}$ and i_a peak H at $E > 0.0\text{ V}$ (Fig. 3). According to Swathirajan only the dissolution of Ni should take place within i_a peak D, but this was not the case, as the dissolution of Zn–Ni alloys took place within i_a peaks D and H. The elemental analysis of Zn–Ni alloy, dissolving in peak D, showed that alloy contained 80.5 at.% Ni and 19.5 at.% Zn. This indicates that the Ni matrix is not oxidized within i_a peak D as stated by Müller et al. [13] and Swathirajan [11], but rather the dissolution of Zn–Ni alloy takes place in i_a peak D instead.

What substance was anodically dissolved within i_a peak H at potentials almost similar to those of Ni dissolution? To

Table 3 Influence of the maximum i_c on Q_D , Q_H and on the total current efficiency (CE_t)

Maximum i_c (A cm^{-2})	0.02	0.03	0.04	0.05	0.1
Q_{cath}/C	1.22	1.42	2.86	2.66	10.04
Q_{anod}/C	0.471	0.645	1.64	1.538	8.55
CE_t (%)	38.5	45.2	56.8	57.8	85.1
Q_D/C (%)	0.46 (97.7)	0.57 (88.4)	0.744 (45.4)	0.588 (38.2)	1.09 (12.75)
Q_H/C (%)	0.011 (2.3)	0.075 (11.6)	0.896 (54.6)	0.95 (61.8)	7.46 (87.3)

The data were obtained under cyclic voltammety conditions ($\nu = 0.005\text{ V s}^{-1}$) at $50\text{ }^\circ\text{C}$

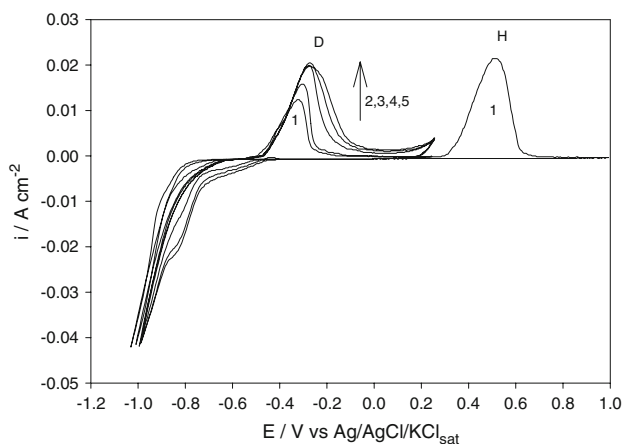


Fig. 6 Cyclic voltammetry ($v = 0.005 \text{ V s}^{-1}$) of Zn–Ni alloy deposited in acetate-chloride plating solution with the ratio $[\text{Zn}^{+2}]/[\text{Ni}^{+2}] = 1:12.8$ at 50°C on Pt electrode pH = 5. (curve 1) first cycle from Pt potential 0.30 to -1.15 V and back to 1.0 V ; (curve 2) second cycle from 1.0 to -1.15 V and back to 0.26 V ; (curves 3–5) third–fifth cycles from 0.26 V to -1.15 back to 0.26 V

find an answer to this question partial potentiodynamic stripping ($v = 0.005 \text{ V s}^{-1}$) in the potential range from $E = -1.15 \text{ V}$ to $E = 0.26 \text{ V}$ (Fig. 6) was performed. This removed the phase dissolved within i_a peak D, whereas the fraction of the alloy, oxidized within i_a peak H, remained. The data show that the substance dissolved in i_a peak H was not pure Ni, but was alloy containing 93.5 at.% Ni ir 6.5 at.% Zn.

Taking into account that the overall composition of the alloy dissolved within i_a peaks D and H was 80.5 at.% Ni and 19.5 at.% Zn and alloy dissolved within i_a peak H contained 93.5 at.% Ni and 6.5 at.% Zn, data obtained at maximum $i_c = 0.05 \text{ A cm}^{-2}$ (Table 3) as well as the total current efficiency = 57.8%, the content of black Zn–Ni alloy dissolved in i_a peak D was calculated. The calculations of the amount of Zn (at.%) in the Zn–Ni alloy phase, dissolved within in anodic current peak D, are presented below. For calculation the data of Table 3 as well as the results of Zn–Ni alloy elemental analysis were used.

1. The amount of Zn present in phase of Zn–Ni alloy, which dissolved within i_a peak D,

$$w_{\text{Zn}}(\text{at.}\%) = Q_{\text{DZn}}/Q_{\text{D}} \times 100;$$

Q_{DZn} , amount of charge which corresponds to anodic dissolution of Zn from Zn–Ni alloy in i_a peak D.

Q_{D} (total anodic charge within peak D) = 0.588 C (Table 3, line 4).

2. $Q_{\text{DZn}} = Q_{\text{Zn}} \times \text{Zn at.}\%$ (within i_a peak D)

Q_{Zn} , amount of charge which corresponds to anodic dissolution of Zn from Zn–Ni alloy within i_a peaks D and H.

Amount of Zn present in Zn–Ni alloy = 19.5 at.%

Q_{anod} (total anodic charge) = 1.538 C (Table 3, line 2)

3. $Q_{\text{Zn}} = Q_{\text{anod}} \times \text{Zn at.}\% = 1.538 \times 0.195 = 0.3 \text{ C}$

Q_{HZn} (amount of charge which corresponds to anodic dissolution of Zn from Zn–Ni alloy in i_a peak H) = $0.95 \text{ C} \times 0.065 = 0.062 \text{ C}$

$Q_{\text{DZn}} = Q_{\text{Zn}} - Q_{\text{HZn}} = 0.3 \text{ C} - 0.062 \text{ C} = 0.238 \text{ C}$

The amount of Zn in phase of Zn–Ni alloy, which dissolved within i_a peak D, $= Q_{\text{DZn}}/Q_{\text{D}} \times 100 = 0.238 \text{ C}/0.588 \text{ C} \times 100 = 40.5 \text{ at.}\%$.

By using the partial potentiodynamic stripping method it was estimated that the phase of white Zn–Ni alloy deposited from solution with the ratio of $[\text{Zn}^{+2}]/[\text{Ni}^{+2}] = 1:4$ at 20°C and dissolved within i_a peak D contained 42.4 at.% Zn and 57.6 at.% Ni [4]. Consequently, data obtained by the partial stripping method showed that the content of Zn–Ni alloy dissolved in i_a peak D was always the same and the content of this alloy was independent of both the ratio of $[\text{Zn}^{+2}]/[\text{Ni}^{+2}]$ and deposition temperature. Analogous data were confirmed by other methods [21, 22]. Analysis of data in the latter part of the chronopotentiograms, obtained by dissolution of the alloy under galvanostatic conditions, and suggests that in this part, corresponding to anodic i_a peak D, the oxidation of Zn–Ni alloy, containing 45.2 wt.% Ni takes place rather than that of the nickel matrix. Data also shows that Zn–Ni alloy, dissolved within i_a peak H and containing 6.5 at.% Zn and 93.5 at.% Ni, provides the black coloration to the coating. The data also indicate that in all potentiodynamic stripping peaks the dissolution of Zn–Ni alloy takes place rather than the Ni matrix being oxidized [11].

4 Conclusions

The phase composition of Zn–Ni alloy deposited under potentiodynamic conditions depends both on the potential sweep rate and the maximum cathodic current density. The quantity of Ni in the alloy increases with increase in both the potential sweep rate and the maximum current density.

The content of Zn–Ni alloy dissolving within i_a peak D is always the same and the content of this alloy is independent of both the ratio of $[\text{Zn}^{+2}]/[\text{Ni}^{+2}]$ in the solution and deposition temperature.

In all potentiodynamic stripping peaks the dissolution of Zn–Ni alloy takes place, rather than the Ni matrix being oxidized.

Zn–Ni alloy, dissolved within i_a peak H and containing 6.5 at.% Zn and 93.5 at.% Ni, provides black coloration to Zn–Ni alloy.

References

1. Hall DE (1983) *Plat Surf Finish* 70(11):59
2. Fabri Miranda FJ, Barcia OE, Diaz SL, Mattos OR, Wiart R (1996) *Eletrochim Acta* 41(7–8):1041
3. Elkhatabi F, Benballa M, Sarret M, Müller C (1999) *Electrochim Acta* 44(10):1645
4. Petrauskas A, Grincevičienė L, Čėsūnienė A, Matulionis E (2005) *Surf Coat Technol* 192:299
5. Alfantazi AM, Page J, Erb U (1996) *J Appl Electrochem* 26:1225
6. Pagotto SO Jr, De Alvarenga Freire CM, Ballester M (1999) *Surf Coat Technol* 122:10
7. Hu C-C, Tsay C-H, Bai A (2003) *Electrochim Acta* 48:907
8. Hu C-C, Bai A (2002) *JEC* 149(11):C615
9. Garcia J, Barcelo J, Sarret M, Müller C, Pregonas J (1994) *J Appl Electrochem* 24:1249
10. Gavrilă M, Millet JP, Mazille H, Marchandise D, Cuntz JM (2000) *Surf Coat Technol* 123:164
11. Swathijaran S (1986) *J Electrochem Soc* 133(4):671
12. Elkhatabi F, Sarret M, Müller C (1996) *J Electroanal Chem* 404(1):45
13. Müller C, Sarret M, Benballa M (2001) *Electrochim Acta* 46(18):2811
14. Stevanovic J, Gojkovic S, Despic A, Obradovic M, Nakic V (1998) *Electrochim Acta* 43(7):705
15. Elkhatabi F, Barcelo G, Sarret M, Muller C (1996) *J Electroanal Chem* 419(1):71
16. Lin Y-P, Selman R (1993) *J Electrochem Soc* 140(5):299
17. Petrauskas A, Grincevičienė L, Čėsūnienė A, Juškėnas R (2005) *Electrochim Acta* 50(5):1189
18. Abd El Rehim SS, Foad EE, Abd El Wahab SM, Hassan Hamdy H (1996) *Eletrochim Acta* 41(9):1413
19. Petrauskas A, Grincevičienė L, Čėsūnienė A, Juškėnas R (2006) *Eletrochim Acta* 51(20):4204
20. Beltowska-Lehman E, Ozga P, Swaitek Z, Lupi C (2002) *Surf Coat Tehnol* 151–152:444
21. Danilov FI, Shevlyakov IA, Sknar TE (1999) *Russ J Electrochem* 35(12):1322
22. Danilov FI, Shevlyakov IA, Sknar TE (1999) *Russ J Electrochem* 35(10):1033